

Radiation hardness of plastic scintillators for the Tile Calorimeter of the ATLAS detector

H Jivan^{1,2}, R Erasmus¹, B Mellado¹, G Peters¹, K Sekonya³ and E Sideras-Haddad^{1,2}

¹ University of the Witwatersrand, 1 Jan Smuts Avenue, Braamfontein 2000, Johannesburg.

² DST-NRF Centre of Excellence in Strong Materials.

³ iThemba LABS. Gauteng.

Email: harshna.jivan@gmail.com

Abstract The Tile Calorimeter of the ATLAS detector employs plastic scintillators to aid in the detection of hadrons, taus, and jets of quarks and gluons that arise from proton-proton collisions within the Large Hadron Collider of CERN. During the first data taking period, plastic scintillators in the GAP region of the detector were exposed to a radiation environment of up to 10 kGy/year. With the LHC set to run proton collisions at almost double the previous centre of mass energy and higher luminosity, the radiation environment is expected to become much harsher. In order to ensure that the radiation damage sustained does not compromise the detector performance, these scintillators will be replaced with more radiation hard plastics. To aid in the choice of scintillator, this preliminary comparative investigation looks into the radiation damage undergone by three polyvinyl toluene (PVT) based plastic scintillators (EJ200, EJ208 and EJ260) provided by ELJEN technology. Samples of each scintillator grade were subject to 6 MeV proton irradiation with doses of the order $O(10^3)$, $O(10^5)$ and $O(10^6)$ Grays using the tandem accelerator of iThemba LABS, Gauteng. Light transmission spectroscopy analysis indicated that a loss of scintillator transparency occurs with increasing irradiation dose, with EJ208 exhibiting the least transmission loss. Raman spectroscopy showed that losses to the benzene ring and vinyl bonding structure occurred for the Mega Gray irradiated samples. This could be correlated with transmission light loss since hydrogen degassing from the breaking of these bonds would result in the formation of free radicals which affect the way in which light is absorbed by the scintillators.

1. Introduction

The Tile Calorimeter of the ATLAS detector, is a hadronic calorimeter responsible for recording the trajectory and energy of hadrons, taus as well as jets of quarks and gluons that result from the proton-proton collisions within the Large Hadron Collider of CERN. Plastic scintillators form an integral component [1] of this calorimeter and are specifically chosen for their properties of high optical transmission and fast rise and decay times. These enable efficient data capture since fast signal pulses can be generated [2]. The main problem encountered by plastic scintillators however, is radiation damage incurred due to their interaction with the ionizing particles to be detected. This damage causes a significant decrease in the light yield of the scintillator and introduces an error into the time-of flight data acquired.

As part of the phase two upgrade of the Tile Calorimeter planned for 2018, a comparative study was conducted into the radiation hardness of several plastic scintillators. The results would aid in choosing the best grade for replacing the current crack scintillators within the Gap region of the Tile Calorimeter. In this paper, we present the results for radiation damage in three polyvinyl toluene based scintillator samples; EJ200, EJ208 and EJ260 obtained from ELJEN technologies [3].

2. Materials and Methodology

The three plastic scintillators under study are composed of a polyvinyl toluene base and 3% of added organic fluors. Differences in the organic fluor dopants give rise to the different characteristic properties observed between the three samples. Some of the characteristic properties are listed in Table. 1 below.

Table 1: Properties of the plastic scintillators as provided from the manufacturers [3].

	EJ200	EJ208	EJ260
Light Output (% Anthracene)	64	60	60
Wavelength of maximum emission (nm)	425	435	490
Rise time (ns)	0.9	1.0	Not available
Decay time (ns)	2.1	3.3	9.2
Refractive index	1.58	1.58	1.58

The tandem accelerator of iThemba LABS in Gauteng was used to irradiate samples with 6 MeV protons. To ensure that the study simulated a similar type of particle-scintillator interaction as observed in the Tile Calorimeter, protons would be required to pass through the samples whilst imparting energy primarily through ionization losses. The stopping range of 6 MeV protons within the scintillator material was determined using the SRIM software package which includes a preset PVT scintillator layer in its materials database [4]. The layer was adjusted to accommodate the CH ratio and density of the plastics as indicated by the manufacturer [3]. The stopping range was found to occur at $\sim 472 \mu\text{m}$. Several samples of each grade were then cut and polished to dimensions of 1 cm by 1 cm, with thickness of $250 \mu\text{m}$. A polishing procedure based on standard metallographic techniques was employed.

Three samples of each scintillator grade were subjected to irradiation with beam intensities of approximately 1 nA and 10 pA with exposure times of 60 min and 6 min in order to achieve radiation doses ranging of the order $O(10^3)$ Grays to $O(10^6)$ Grays. Samples were mounted in a hexagonal sample carousel and housed within the microprobe chamber. The beam current was determined by measuring the charge across a metal plate situated on the side opposite to the sample on the carousel. The beam was scanned in the x and y plane using a uniform raster-scan pattern to achieve an irradiated area of approximately 4 mm by 4 mm. After irradiation, samples were contained in vials that were wrapped in aluminium foil. This was done in order to prevent the recovery of damage through photo-bleaching effects that result from exposure to visible light.

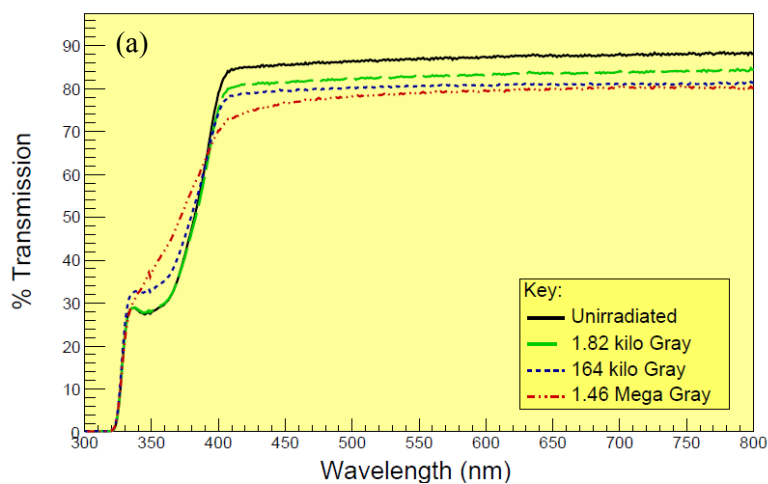
Transmission spectroscopy was conducted using the Varian Carry 500 spectrophotometer. Light transmission was measured relative to transmission in air over a range of 300-800 nm. Thereafter, the Raman spectra for un-irradiated and the highest dose irradiated samples were obtained using the Horiba Jobin-Yvon Raman spectrograph. An Argon laser was used to provide a 515 nm excitation wavelength. The Raman analysis was used to provide information on changes to the bonding structure induced by radiation damage.

3. Light Transmission Results and Analysis

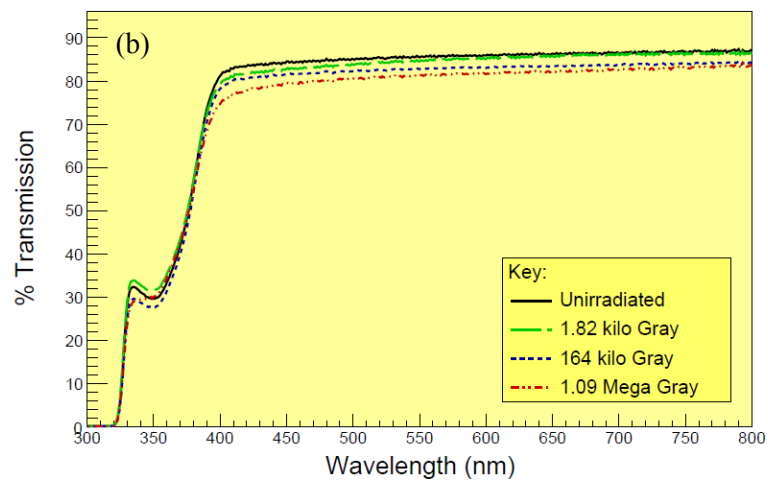
The results of light transmission spectroscopy for each grade relative to light transmission in air are shown in figure 1. The absorptive edge completely falls away by 320 nm in both EJ200 and EJ208, whilst this occurs at 340 nm for EJ260. It is observed that the overall transmission decreases as dose exposure increases. An increase in transmission within the region of 340 nm to 380 nm is observed prominently within EJ200 and could indicate damage to the fluorescent dyes. Furthermore, an absorptive tint is observed to form along the absorptive edge in EJ260 which shifts towards higher wavelengths as dose increases. This could either indicate the formation of free radicals or the development of a competing absorptive process between the primary and secondary fluor dopants. This additional absorption component may reduce the attenuation length of the scintillation light as described [5].

We consider the transmission loss at a wavelength of approximately 450 nm as this corresponds to the peak absorption wavelength of the fiber that these scintillators are coupled to within the Tile Calorimeter. For dose exposure in the range of Mega Grays, 9.8% light transmission loss is observed in EJ200, whilst EJ260 shows an 8% loss and EJ208 shows a 5.5% loss. At this dose, visible yellowing of the samples occur within the irradiated region. A systematic error of 3% in the transmission loss arose due to slight changes of sample position on the sample mount within the spectrophotometer upon repetition of experiments.

Transmission vs Wavelength For EJ200 at different Exposure Doses



Transmission vs Wavelength For EJ208 at different Exposure Doses



Transmission vs Wavelength For EJ260 at different Exposure Doses

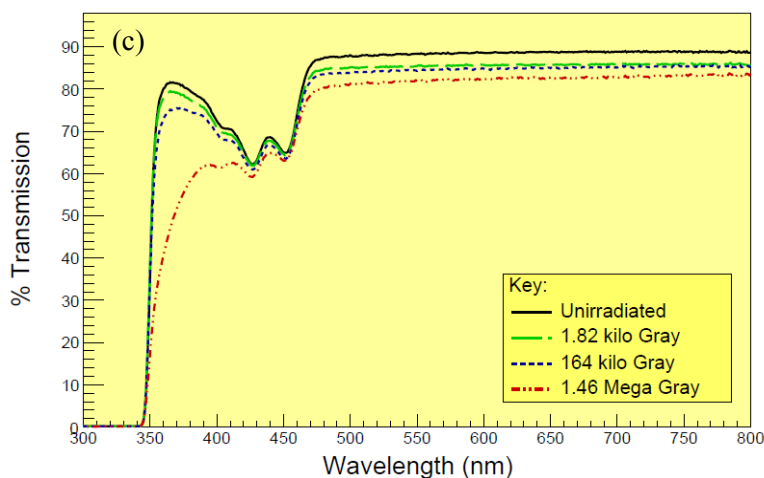


Figure 1: Transmission spectrum for un-irradiated and irradiated samples over several doses relative to air for (a) EJ200, (b) EJ208 and (c) EJ260.

4. Raman Spectroscopy Results and Analysis

Raman spectra were obtained for un-irradiated and Mega Gray dose irradiated samples of each grade. An increased amount of background fluorescence could be observed in the radiation damaged samples which may arise from free radicals interacting with the excitation light. It should be noted that transmission spectra also indicate a loss in scintillator transmission at this excitation wavelength of 515 nm. EJ260 had the most drastic occurrence of background fluorescence as it is a green emitting scintillator and absorbs light at higher wavelengths as compared to EJ200 and EJ208. Plots of the Raman spectra after subtraction of the fluorescent background are shown in figure 2. The Raman peaks observed were then allocated to the characteristic functional groups or vibrational groups using the Raman Peak assignment datasheet [6]. The peak assignment is summarized in table 2. In order to assess change to the bonding structure and minimize errors caused from fluctuations in laser intensity and background subtraction, the ratio of the intensity of each peak to the intensity of a control peak on each of their respective spectra were plotted as shown in figure 3. Comparing changes to these ratios then gave an indication to the relative increase or decrease to that particular bonding structure.

Table 2: Allocation of peaks to characteristic functional groups or vibrational groups.

Functional Group/Vibration	Peak Assignment for EJ200 and EJ208	Peak assignment for EJ260
$\delta(\text{C-C})$ aliphatic	1-2	1
$\nu(\text{C-C})$ alicyclic or aliphatic chain vibrations	3-5, 7-9	2-4, 6-7
$\nu(\text{C-C})$ aromatic ring chain vibrations	6	5
$\delta(\text{CH}_3)$	10	/
$\delta(\text{CH}_2)$ or $\delta(\text{CH}_3)$ asymmetric	11	8
$\nu(\text{C=C})$	12	9
$\nu(\text{C-H})$	14	11-12
$\nu(=\text{C-H})$	15	13-14
Control peak	13	10

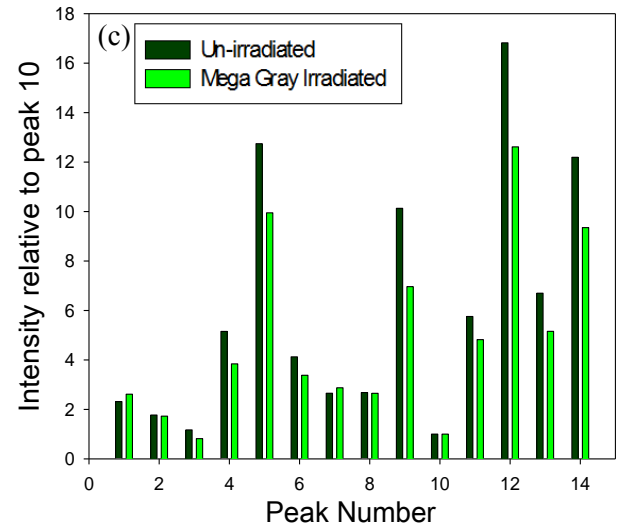
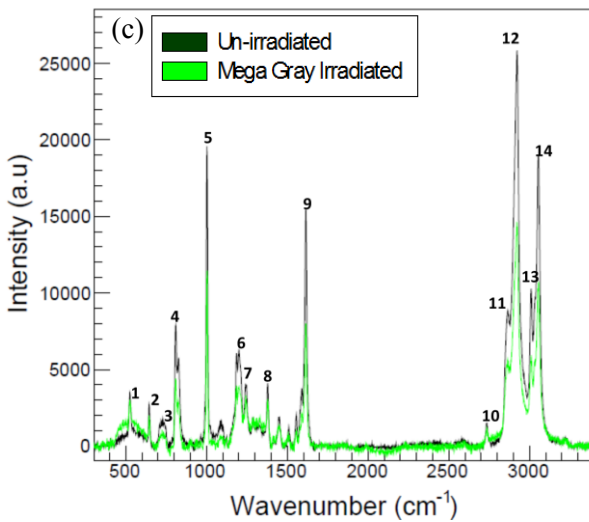
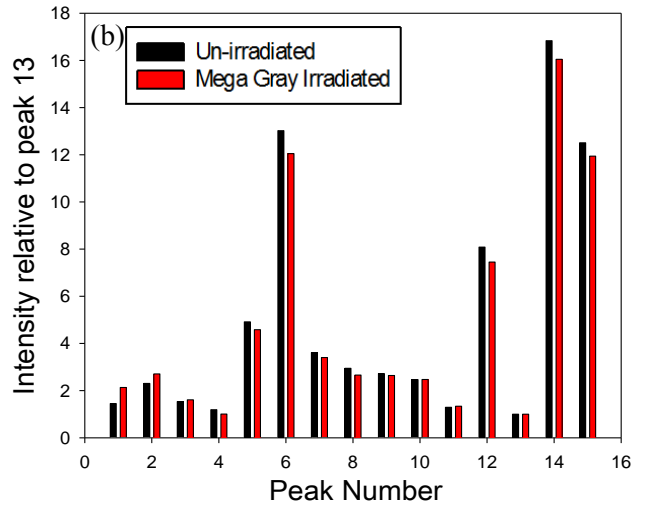
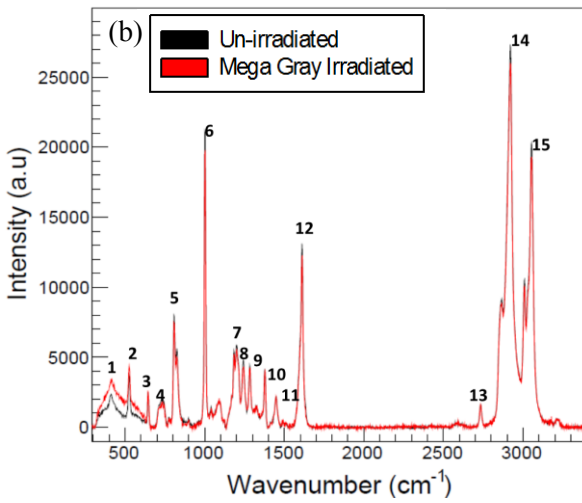
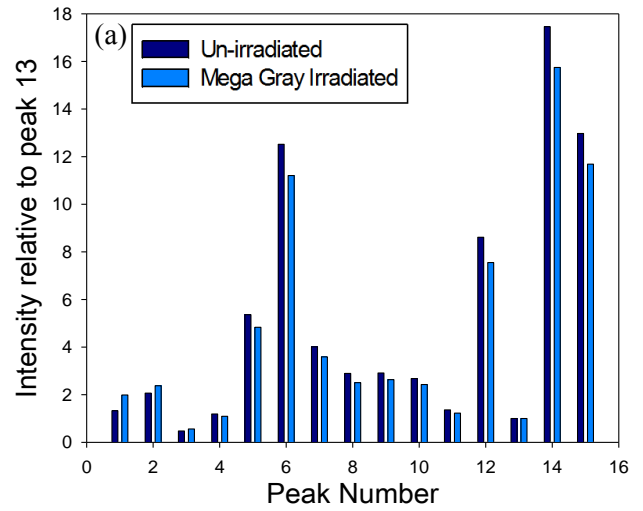
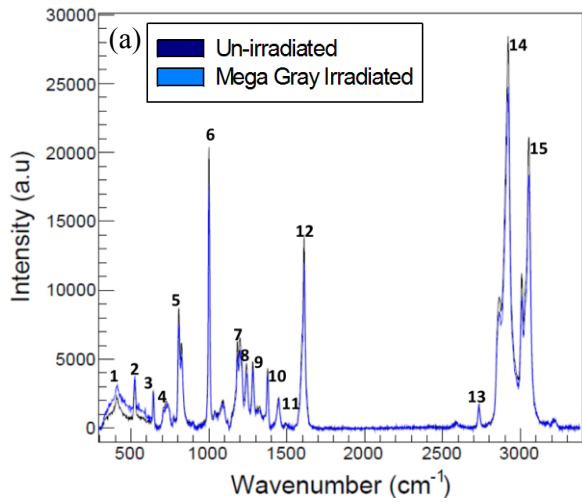


Figure 2: Background subtracted Raman spectra for (a) EJ200, (b) EJ208 and (c) EJ260.

Figure 3: Plots of intensity ratios between peaks and control peak for (a) EJ200, (b) EJ208 and (c) EJ260.

The spectra for irradiated and un-irradiated samples are fairly similar, with a few subtle changes. No broadening of peaks or the formation of new peaks were observed. All three samples show an increase in the C-C aliphatic or alicyclic vibrations indicated by peaks 1 and 2 in EJ200 and EJ208, and peaks 1 and 7 in EJ260. These bonds occur in chains not belonging to the aromatic benzene ring structure. All the other peaks show a decrease, with the most prominent occurring for peaks 6, 12, 14 and 15 in EJ200 and EJ208 and peaks 4, 5, 9 and 11-14 in EJ260. These typically represent the C-C aromatic ring bonds, as well as C=C, C-H and =(C-H) which could belong to either the benzene ring or the vinyl backbone. Damage to the benzene ring structure directly affects the scintillation mechanism which would lead to a degradation in scintillation light yield. The Mega Gray irradiated doses of each scintillator grade contain more carbon type species and less hydrogen type species than the un-irradiated samples. This indicates that hydrogen degassing occurs when the C-H bonds are broken.

5. Conclusions

According to the results found during this investigation, exposure to proton irradiation leads to a decrease in light transmission as radiation dose exposure is increased. Overall, EJ200 exhibited the most loss in transparency at a wavelength of 450 nm when irradiated with a Mega Gray range dose, and EJ208 showed the least transmission loss. Although EJ260 showed less transmission loss than EJ200 at 450 nm, the development of an absorptive tint shift could indicate additional damage effects such as free radical formation. Other features observed on the spectra such as the formation of additional transmission peaks and dips indicate that radiation damage could be affecting the light transfer mechanism. This would greatly affect the scintillator light conversion efficiency and hence light yield studies will need to be conducted.

Surface scratches and structural damage caused during the sample preparation procedure could have caused minor additional transmission loss and therefore provide an experimental error. The extent of this random error could not be gauged accurately as each sample was polished separately and most of this damage was not directly visible to the naked eye. A more gentle polishing procedure incrementing over more polishing stages and finishing with a finer polishing stage, as well as using a larger sample group could reduce this effect in future studies conducted. It would also be imperative that transmission tests are conducted on individual samples before and after irradiation as opposed to comparing transmission of irradiated samples to that of an un-irradiated control sample.

Raman analysis indicates that structural changes occur within the samples. The species of C-C aromatic, C=C, C-H and =(C-H) bonds in the benzene ring structure and vinyl backbone decrease whilst a small amount of additional C-C aliphatic bonds are formed when the scintillators are exposed to a dose in the Mega Gray range. This indicates that hydrogen degassing occurs and the damaged scintillators become more carbon rich. The observation of an increased background fluorescence in the Raman spectra of the Mega Gray irradiated samples of each grade is further indicative of free radical formation. This is particularly emphasized in EJ260.

From this preliminary study, EJ208 appears as a good potential candidate as it suffers the least transmission loss and structural differences in its Raman spectra are less apparent than in EJ200 and EJ260, however further investigation is required. This study has provided a good baseline for the experimental techniques required for investigating the radiation damage of plastic scintillators and improvements will be implemented for further studies to come.

6. Upcoming work

Several scintillator samples obtained from Bicon, the Joint Institute for Nuclear Research (Dubna) as well as samples manufactured particularly for the Tile Calorimeter in Protvino, will be added to the study. New samples have been polished to dimensions of 5 mm x 5 mm x 0.35 mm to prevent inhomogeneity resulting from machining stress. An analysis of the changes in light response toward beta electrons from a strontium source is underway. Light transmission and light yield testing after

irradiation will be conducted at several times over the course of a year in order to establish long term changes to the optical properties due to the chemical reactions which may arise from free radical interactions with the environment. A larger sample group will be looked at with several samples being irradiated per dose in order to ensure repeatability in the effects observed. Electron paramagnetic resonance studies conducted by C. Pelwan *et al.* [7] are also underway in order to determine types of free radical species that may form as a result of radiation damage. An investigation into the damage undergone by previous scintillator tiles used within the Tile Calorimeter during the previous data taking period at ATLAS is also ongoing by L. Maphanga, *et al.* [8].

7. References

- [1] ATLAS Collaboration 2008 *The ATLAS Experiment at the CERN Large Hadron Collider* (IOP Publishing and SISSA)
- [2] Knoll G F 1999 *Radiation Detection and Measurement, Third Edition* (Michigan: John Wiley & Sons Inc.) chapter 8 pp 220-222
- [3] ELJEN Technology 2013 *Products: Plastic Scintillators* [Online]. Available: <http://www.eljentechnology.com/index.php/products/plastic-scintillators>.
- [4] Ziegler J 2013 *SRIM and TRIM : Particle interactions with matter* [Online]. Available: <http://www.srim.org>.
- [5] Zorn C 1993 A pedestrian's guide to radiation damage in plastic scintillators *Radiat. Phys. Chem.* **41** 37-43
- [6] G. Socrates 2004 *Infrared and Raman Characteristic Group Frequencies Tables and Charts, Third Edition*, (London:John Wiley and Sons) pp 35-47
- [7] Pelwan C, *et al.* 2014 *Electron Paramagnetic Resonance Analysis of Plastic Scintillators for the Tile Calorimeter of the ATLAS detector* (submitted to the SAIP 2014 Conference)
- [8] Maphanga L, *et al.* 2014 *Characterization of Damage in in-situ Radiated Plastic Scintillators at the Tile Calorimeter of ATLAS* (submitted to the SAIP 2014 Conference)